WARSAW UNIVERSITY OF TECHNOLOGY Index 351733
FACULTY OF CIVIL ENGINEERING
COMMITTEE FOR CIVIL AND WATER ENGINEERING
POLISH ACADEMY OF SCIENCES ISSN 1230-2945
DOI: 10.24425/ace.2024.150974
ARCHIVES OF CIVIL ENGINEERING
Vol. LXX ISSUE 3 2024
pp. 117 –137

Research paper

Rotational restraint of cold-formed Z-purlins given by the trapezoidal sheeting with additional stiffening ribs

Michał Gajdzicki[1]

Abstract: The Eurocode 3-1-3 [1] provisions, according to which the rotational restraint of a cold-formed Z-purlin given by the sheeting has to be determined, set out guidelines for the first-generation trapezoidal sheets only in strictly defined cases, and for the second-generation sheets there are no guidelines at all. In the experimental tests presented in this paper, values of stiffness C_D were determined in the case where trapezoidal sheeting with additional stiffening ribs in the middle of each trough was used. Then, the obtained values were confirmed by numerical simulations. The cases when fasteners are located in each trough next to the intermediate stiffener (the 1+1 arrangement) or near the trapezoidal sheeting webs in every second trough (the 2+0 arrangement) were analyzed. Values of stiffness C_D obtained from the experiments were also compared with C_D values obtained on the basis of the Eurocode 3-1-3 provisions. As a result of the analyses carried out, several changes to the Eurocode 3-1-3 provisions were proposed. Values of the rotational coefficient C_{100} for cases not covered by Eurocode 3-1-3 were presented and, in addition, a modification of this coefficient for the 1+1 fastener arrangement under gravity loading was proposed.

Keywords: cold-formed Z-purlin, sheet-to-purlin fastener, stiffness C_D, rotational restraint

[1] PhD., Eng., Lodz University of Technology, Faculty of Civil Engineering, Architecture and Environmental Engineering, Al. Politechniki 6, 93-590 Lodz, Poland, e-mail: michal.gajdzicki@p.lodz.pl, ORCID: 0000-0003-0555-1648

1. Introduction

The profiled trapezoidal steel sheeting attached to cold-formed Z-purlins is commonly used in roofing systems. The development of steel sheet profiling technology has resulted in the introduction of trapezoidal sheets with more and more complicated cross-sections in which there are numerous stiffening ribs (a second-generation profile). However, this development is not followed by the code provisions included in Eurocode 3-1-3 [1], according to which the rotational restraint of a cold-formed purlin given by the sheeting has to be determined. These regulations not only lack any guidelines for second-generation trapezoidal sheets, but are also very limited for those without the additional stiffeners (first-generation sheets). Unfortunately, this leads to situations in which designers of steel structures have to ignore the limitations of the rules described therein, not being sure whether the calculated value of buckling resistance of cold-formed Z-purlins is correct.

Investigations on the behaviour of restrained cold-formed purlins have been carried our since 90. of the previous century, in the US by Pekoz and then continued by Schafer [2], as well as parallelly conducted in Australia by Hancock [3,4] and his co-researchers. In Poland, the practical application of the results mentioned above had been implemented in the book [5], that was next substituted by the implementation of the Eurocode 3-1-3 [1].

The first recommendations for determining the stiffness C_D were presented in ENV 3-1-3 [6] and were the result of experiments described by Lindner and Gregull in [7–9] with later modifications proposed by Lindner and Groeschel in [10, 11]. Unfortunately, the applicability of these provisions was strongly limited to specific diameters of fasteners and steel washers or the nominal core thickness of steel sheeting used in the experimental tests mentioned above. In the final version of Eurocode 3-1-3, an extended formula developed by Vrany [12, 13] was proposed, with several coefficients depending on the sheet-to-purlin connection geometry.

Later, Gajdzicki and Goczek [14, 15] presented the results of numerical simulations, on the basis of which it was proved that the diameter of the sheet-to-purlin fasteners does not have such a big impact on the value of the final rotational restraint C_D and that this limitation can be removed from the code provisions. Wang, Zhang, Yang, Bai and Ren conducted a parametric studies in [16] based on the validated model to investigate the influences of geometric dimensions on the rotational stiffness. The authors proposed two modified coefficients for calculating the rotational stiffness based on the codified formulae in [1], where the effect of the wall thickness and the flange width of the purlin are both considered. Other parameters, such as the effect of anti-sag bars, rib spacing and wave height on the failure modes and ultimate capacity of C-purlins restrained by the sheeting connected with self-drilling screws, were discussed in [17].

For the first time, studies in which a different arrangement of sheet-to-purlin fasteners was used were described in [18]. The case where two fasteners were located near the trapezoidal sheeting webs in every second trough was analyzed and it was proved that such a fastener arrangement, in negative positioning of the trapezoidal sheeting, gives even more than twice higher rotational restraint of Z-purlins provided by the sheeting. However, these tests were limited to the first-generation steel trapezoidal sheeting only, i.e. with no additional ribs along the forming fold. In this paper, the second-generation steel sheeting was used in the tests, in

which, due to the ribs in the middle of the trough width, the use of two fasteners near the webs is particularly justified. Similar guidelines for determining the rotational restraint of cold-formed purlins given by sandwich panels were provided by Balazs [19] and Ciesielczyk [20].

A study on the impact of the screw location and the diaphragm effects on the buckling behaviour of the simply supported C/Z-section purlins under wind uplift loadings was presented by Yang and Bai in [21]. The diaphragm effects provided by the sheeting and the warping-torsional effect induced by load eccentricity ware taken into account in the differential equations of the nonlinear twisting flexural-torsional model. The relationship between the buckling load and rotational restraint stiffness was also provided. Similar analyses were presented by Zhao, Yang, Wang and Chan in [22] where a series of torsional restraint tests (F-tests) for both sigma and zed sections were performed. The rafter-purlin connection flexibility, and its influence on the stressed skin effect of the corrugated sheet claddings was also analyzed in [23] for cold-formed purlins with overlaps.

A numerical investigation into the buckling behaviour of cold-formed steel zed purlins when subjected to transverse distributed uplift loading were presented by Ren, Zhao and Chen in [24]. The study used both linear and non-linear finite element methods to investigate the pre-buckling, buckling and post-buckling behaviour of zed-section purlins in purlin-sheeting systems. Influences of boundary conditions and restraints from sheeting on web shear buckling, local, distortional and lateral-torsional buckling behaviour, and the buckling interactions of the purlins are discussed. Similar issues were analyzed by Reszut, Szewczak, Różyło and Guminiak in [25], where local and global instability behaviour was investigated using linear buckling analysis and the models were verified by the comparison with theoretical critical bending moment obtained from the analytical formulae based on the Vlasow beam theory of the thin-walled elements.

2. Eurocode 3-1-3 guidelines for determining C_D values

As mentioned above, in a limited number of cases the rotational stiffness C_D of the connection between the sheeting and the purlin can be determined from the formulas in Section 10.1.5.2 of Eurocode 3-1-3 1 [1]. Moreover, the stiffness C_D can be also determined from a very simple formula ($130p$) in which the stiffness depends only on p, i.e. the number of sheet-to-purlin fasteners per meter length of purlin. Due to its simplicity, this formula is more often used. However, it gives results always on the unsafe side, which was shown in [14], and therefore it should be removed from Eurocode 3-1-3.

In design situations in which geometric limitations specified in Eurocode 3-1-3 are not satisfied, which happens quite often, the C_D value should be calculated from Eq. (2.2). However, in these cases it is required to determine the experimental value of the lateral spring stiffness K. Two test set-ups with different static schemes and the procedure for the experimental determination of the stiffness K are described in Annex A of Eurocode 3-1-3. In this study, the test set-up shown in Fig. 1 and 4 was used.

In accordance with the Eurocode 3-1-3 provisions, the measured linear displacement δ of the upper flange in the direction of the force F depends on the flexibility of two types:

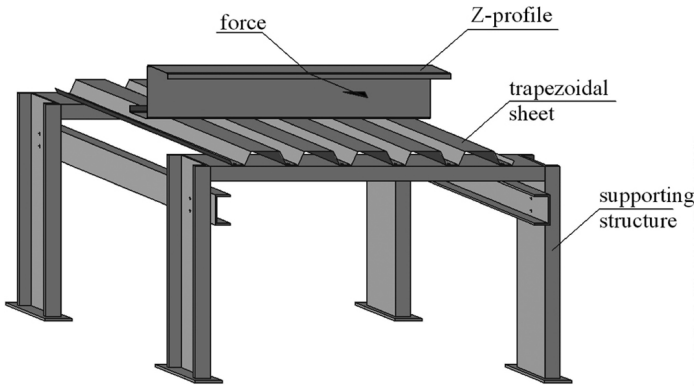

Fig. 1. The scheme of the test set-up used

the connection between the purlin and the sheeting $(1/K_A)$ and the distortion of the purlin cross-section $(1/K_B)$. The value of the force F in Eq. (2.1) is the load per unit length of the test specimen that produces a lateral deflection of $\delta = h/10$, where h is the height of the purlin cross-section.

$$\frac{1}{K} = \left(\frac{1}{K_A} + \frac{1}{K_B}\right) = \frac{\delta}{F} \tag{2.1}$$

If the lateral spring stiffness K per unit length is obtained by testing, the value of the total rotational spring stiffness C_D for gravity and uplift loading should be determined from:

$$C_D = \frac{1}{\dfrac{1}{K} - \dfrac{1}{K_B}} h^2 = K_A h^2 \tag{2.2}$$

In the above equation the lateral stiffness due to the distortion of the purlin cross-section K_B is known and depends on the material constants (E, ν), the geometric dimensions of the cross-section (t, h, h_d) and the location of the fastener in the width of the purlin flange (a, b). In the case of the uplift loading the K_B value should be determined from Eq. (2.3) and in the case of the gravity loading from Eq. (2.4).

$$K_B = \frac{Et^3}{4\left(1-\nu^2\right) h^2 \left(h_d + a\right)} \tag{2.3}$$

$$K_B = \frac{Et^3}{4\left(1-\nu^2\right) h^2 \left(h_d + 2a + b\right)} \tag{2.4}$$

It should be noted that although the test set-up recommended by Eurocode 3-1-3 is not complicated, in engineering practice it is too expensive and time-consuming to perform tests only to determine the necessary stiffness C_D that is needed afterwards to calculate the buckling resistance of cold-formed Z-purlins restrained by trapezoidal sheeting. In such a situation, designers will rather use the proposed formulas, ignoring their significant limitations.

3. The aim of the research

The author [18] showed that the use of two sheet-to-purlin fasteners in every second trough of a trapezoidal sheet results in higher values of the rotational stiffness C_D. However, in those studies, only first-generation trapezoidal sheets were used, where all cross-section walls were flat. In the experimental tests described here, second-generation trapezoidal sheeting with stiffening ribs on webs and a wider flange was used. In Eurocode 3-1-3, it is recommended that the trapezoidal sheeting should provide a full continuous lateral restraint to the purlins, when it is fastened using self-tapping screws in every or every second trough of the sheet. In the second case, the sheeting provides five times smaller shear stiffness (0,2S). In the case of second-generation trapezoidal profiled sheets, where there is an internal stiffener in the middle of the trough, it is necessary to move the fastener to one side or the other. Therefore, in this study, it was decided to analyze the differences in the rotational stiffness C_D given to the Z-purlin when the fastener is in each trough next to the intermediate stiffener (the 1+1 arrangement) or is located near the trapezoidal sheeting webs in every second trough (the 2+0 arrangement) – see Fig. 2. Due to a low bending stiffness of a steel troughed sheet, it seems reasonable to locate the fasteners near the webs. The external load applied to the free flange of the Z-profile is transferred to the sheeting a shorter way. That significantly reduces the deformation of the connection, which consequently increases the value of the lateral stiffness K_A and the stiffness C_D.

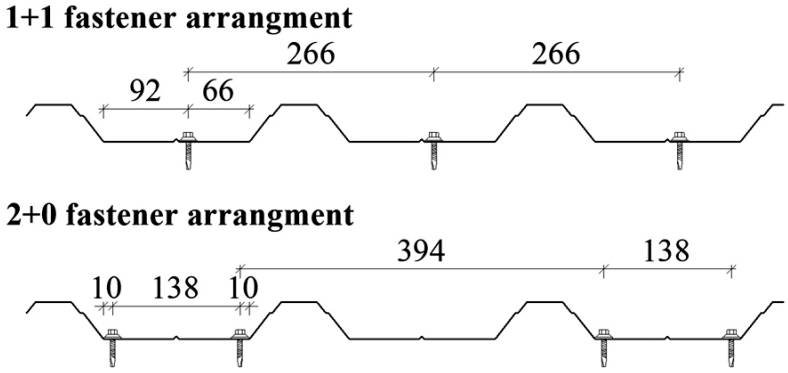

Fig. 2. The arrangement of the sheet-to-purlin fasteners

In order to confirm the above thesis and investigate the influence of the arrangement of fasteners on the value of the rotational stiffness C_D, 48 test specimens were built varying with respect to the following parameters:

- trapezoidal sheeting geometry (T40 × 0.5; T40 × 0.7; T50 × 0.5) – see Fig. 3,
- width of the purlin flange connected to the sheeting (60 or 68 mm) – see Fig. 3,
- the arrangement of fasteners (1+1; 2+0) – see Fig. 2,
- load direction (U – uplift; G – gravity).

Figure 3 shows geometric dimensions of cross-sections of the trapezoidal sheets and the purlins measured in the midline. In the experimental tests, fasteners with a diameter of

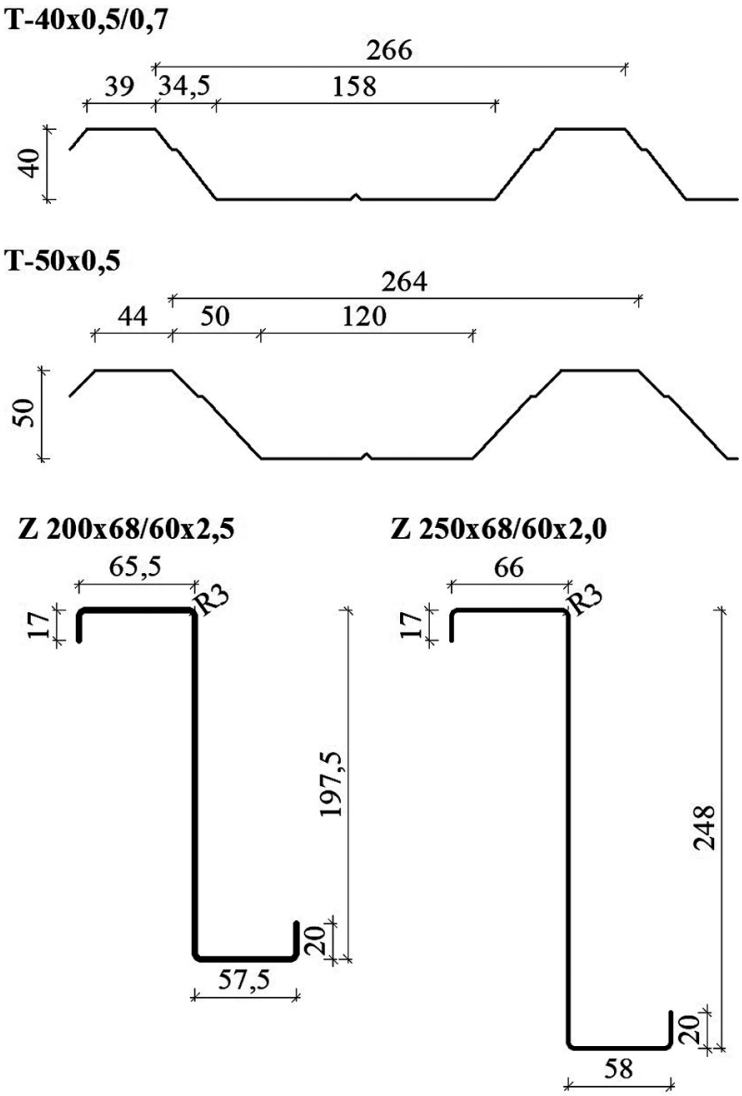

Fig. 3. Geometry of trapezoidal sheets and Z-profiles – midlines

5.0 mm and sealing washers with a diameter of 14 mm were used. The fasteners were located at a distance of 10 mm from the intermediate stiffener of the sheeting trough in the 1+1 arrangement and 10 mm from the webs of the trapezoidal sheet in the 2+0 arrangement (Fig. 2). In the other direction, the fasteners were always located in the half-width of the purlin flange. The description of all 24 models tested under gravity (G) and uplift (U) load conditions is presented in Table 1. The number in brackets in purlin designations denotes the width of the contact zone between the trapezoidal trough and the upper purlin flange.

Table 1. Test specimen

Test specimen	Trapezoidal sheeting	Purlin	Fastener arrangement	Load direction
(1)	(2)	(3)	(4)	(5)
1	T40 × 0.5	Z200 × 2.5(68)	1+1	G/U
2	T40 × 0.5	Z200 × 2.5(68)	2+0	G/U
3	T40 × 0.5	Z200 × 2.5(60)	1+1	G/U
4	T40 × 0.5	Z200 × 2.5(60)	2+0	G/U
5	T40 × 0.5	Z250 × 2.0(68)	1+1	G/U
6	T40 × 0.5	Z250 × 2.0(68)	2+0	G/U
7	T40 × 0.5	Z250 × 2.0(60)	1+1	G/U
8	T40 × 0.5	Z250 × 2.0(60)	2+0	G/U
9	T40 × 0.7	Z200 × 2.5(68)	1+1	G/U
10	T40 × 0.7	Z200 × 2.5(68)	2+0	G/U
11	T40 × 0.7	Z200 × 2.5(60)	1+1	G/U
12	T40 × 0.7	Z200 × 2.5(60)	2+0	G/U
13	T40 × 0.7	Z250 × 2.0(68)	1+1	G/U
14	T40 × 0.7	Z250 × 2.0(68)	2+0	G/U
15	T40 × 0.7	Z250 × 2.0(60)	1+1	G/U
16	T40 × 0.7	Z250 × 2.0(60)	2+0	G/U
17	T50 × 0.5	Z200 × 2.5(68)	1+1	G/U
18	T50 × 0.5	Z200 × 2.5(68)	2+0	G/U
19	T50 × 0.5	Z200 × 2.5(60)	1+1	G/U
20	T50 × 0.5	Z200 × 2.5(60)	2+0	G/U
21	T50 × 0.5	Z250 × 2.0(68)	1+1	G/U
22	T50 × 0.5	Z250 × 2.0(68)	2+0	G/U
23	T50 × 0.5	Z250 × 2.0(60)	1+1	G/U
24	T50 × 0.5	Z250 × 2.0(60)	2+0	G/U

4. Results of the experimental tests

The test set-up used in the experimental test was the same as the one described in [18]. In order to avoid the initial rotation of the connection due to the self-weight of the Z-profile, the test set-up was placed horizontally, not vertically as in the studies described in [12]. For this reason, the purlin free flange was loaded horizontally with the use of a block mounted at a required height on a cantilever (Fig. 4).

Fig. 4. The 13U specimen under uplift load

The load was applied in increments of about 20 N/min. The linear displacement of the Z-profile free flange was read from a digital linear displacement sensor. The load was increased until the required lateral displacements of the free flange ($\delta = h/10$) were achieved. The final values of the forces F are given in column (2) in Table 2 for gravity loading and in Table 3 for uplift loading. Afterwards, by substituting the obtained values of the force F and the displacement δ into Eq. (2.1), the total lateral spring stiffness K per unit length was calculated. Therefore, as the lateral spring stiffness K per unit length was obtained by testing (column (3)), and the values of K_B were calculated for each Z-profile (column (4)), it was possible to determine the value of the lateral stiffness corresponding to the rotational stiffness of the joint between the sheeting and the purlin K_A (column (5)). Finally, the value of the total rotational spring stiffness C_D for gravity and uplift loading could be determined from Eq. (2.2) (column (6)). It should be noted here that the K_B values were divided by the length of the test specimen, i.e. the distance between the external fasteners, which was 0.798 m for the 1+1 arrangement and 0.532 m for the 2+0 arrangement.

Table 2. Experimental results for gravity loading

Test specimen	F **[N]**	K **[N/mm]**	K_B **[N/mm]**	K_A **[N/mm]**	$C_{D,\mathrm{EXP}}$ **[Nm/m]**	**Ratio**
1G	149.9	7.49	83.99	8.23	329	2.93
2G	405.2	20.26	125.99	24.14	966	
3G	161.4	8.07	88.30	8.88	355	1.85
4G	292.3	14.61	132.44	16.43	657	
5G	109.9	4.40	23.29	5.42	339	1.85
6G	194.4	7.77	34.94	10.00	625	
7G	110.8	4.43	24.32	5.42	339	1.67
8G	181.0	7.24	36.47	9.04	565	

Continued on next page

Table 2 – *Continued from previous page*

Test specimen	F **[N]**	K **[N/mm]**	K_B **[N/mm]**	K_A **[N/mm]**	$C_{D,\mathrm{EXP}}$ **[Nm/m]**	**Ratio**
9G	287.5	14.37	83.99	17.34	694	1.73
10G	484.9	24.25	125.99	30.02	1201	
11G	214.2	10.71	88.30	12.19	488	1.63
12G	345.9	17.30	132.44	19.90	796	
13G	176.4	7.06	23.29	10.13	633	1.79
14G	298.0	11.92	34.94	18.09	1131	
15G	179.8	7.19	24.32	10.21	638	1.95
16G	322.3	12.89	36.47	19.94	1246	
17G	178.9	8.94	84.63	10.00	400	2.13
18G	364.2	18.21	126.95	21.26	850	
19G	153.6	7.68	88.96	8.40	336	1.83
20G	275.8	13.79	133.45	15.38	615	
21G	106.4	4.26	23.47	5.20	325	2.36
22G	227.7	9.11	35.20	12.29	768	
23G	95.1	3.81	24.50	4.51	282	2.13
24G	190.3	7.61	36.75	9.60	600	

Table 3. Experimental results for gravity loading

Test specimen	F **[N]**	K **[N/mm]**	K_B **[N/mm]**	K_A **[N/mm]**	$C_{D,\mathrm{EXP}}$ **[Nm/m]**	**Ratio**
1U	197.1	9.85	119.84	10.74	429	2.04
2U	390.3	19.52	179.75	21.89	876	
3U	184.2	9.21	121.95	9.96	398	2.07
4U	371.3	18.56	182.93	20.66	826	
5U	141.4	5.66	31.50	6.89	431	2.09
6U	275.8	11.03	47.25	14.39	900	
7U	139.2	5.57	31.95	6.74	421	2.11
8U	274.5	10.98	47.93	14.24	890	
9U	294.7	14.74	119.84	16.80	672	1.70
10U	491.7	24.59	179.75	28.48	1139	
11U	229.6	11.48	121.95	12.68	507	1.96
12U	436.9	21.84	182.93	24.81	992	
13U	202.1	8.08	31.50	10.87	680	1.90
14U	359.0	14.36	47.25	20.63	1289	

Continued on next page

Table 3 – *Continued from previous page*

Test specimen	F [N]	K [N/mm]	K_B [N/mm]	K_A [N/mm]	$C_{D,\mathrm{EXP}}$ [Nm/m]	Ratio
15U	210.0	8.40	31.95	11.39	712	1.37
16U	294.7	11.79	47.93	15.64	977	
17U	243.9	12.20	120.74	13.57	543	1.74
18U	416.9	20.84	181.12	23.55	942	
19U	198.3	9.91	122.88	10.78	431	1.98
20U	383.1	19.15	184.32	21.37	855	
21U	163.5	6.54	31.74	8.24	515	1.91
22U	296.0	11.84	47.60	15.76	985	
23U	144.2	5.77	32.19	7.03	439	2.21
24U	294.1	11.76	48.29	15.55	972	

The ratio of the stiffness C_D obtained for the 2+0 fastener arrangement to the one obtained for the 1+1 arrangement in the test set-up with the same trapezoidal profiled sheets and purlin profiles is shown in the last column of Tables 2 and 3.

5. Verification of the results

In the further part of the research, a numerical model was built using a non-linear FEA model described in [15, 18], which was validated based on the obtained experimental results. Similar numerical models were used in the analyses described in [16, 17]. The geometry of the finite element model was based on the center line of Z- and sheet profiles (Fig. 3).

The profile section and the trapezoidal sheet were discretized using a linear 4-node quadrilateral S4R thick-shell element from the Abaqus finite element library. This element has six degrees of freedom per node utilizing the reduced integration. In all numerical simulations, a 5-mm finite element mesh was used for both the trapezoidal sheet and the Z-profile section. The size of the finite element was determined on the basis of the convergence study. The master-slave surface pair option was used to model the contact between the Z-profile flange (master) and the sheeting trough (slave). Each fastener between the sheeting and the Z-profile flange was idealized as four connector elements (all six degrees of freedom constrained) spaced evenly around a hole with a diameter of 5.0 mm. In order to determine the exact material characteristics of steel, three static tensile tests were performed on samples taken from the Z-profiles and the trapezoidal sheet. Therefore, actual values of the stress-strain relationship were entered in the Abaqus software. At the extreme edge of each trough of the trapezoidal sheeting, three linear displacements were constrained, while the rotation was left free. In order to obtain the required displacement, the load was applied to the free flange of the Z-profile section in several increments. The load direction always remained parallel to the sheeting and independent of deformation. The two directions of loading were applied to reflect the uplift and gravity loading.

All results from numerical simulations corresponding to the experimental tests are presented in Table 4 for gravity loading and in Table 5 for uplift loading. To determine the final value of the rotational spring stiffness C_D, the same procedure was used as the one described in the previous section concerning the experimental results.

The ratio of the value obtained in the experimental tests to the value from the numerical simulation is given in both tables in column (7). It can be concluded that the convergence of these results is very good, as the average ratio is 1.10 for gravity loading and 0.92 for uplift loading.

Collecting the values of the lateral displacement of the free flange δ after each increment of the load F made it possible to chart the relationship between load and displacement for each model. Figures 5 and 6 compare the relationships obtained from numerical simulations (dashed line) with those from experimental tests (solid line).

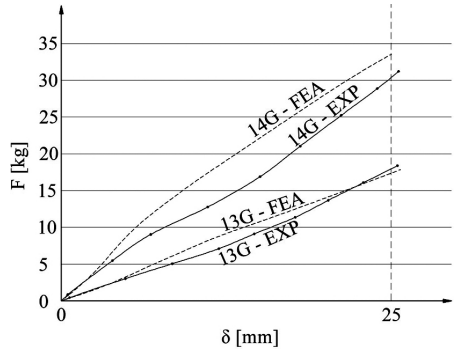

Fig. 5. Load-displacement relationship for specimens 13G and 14G

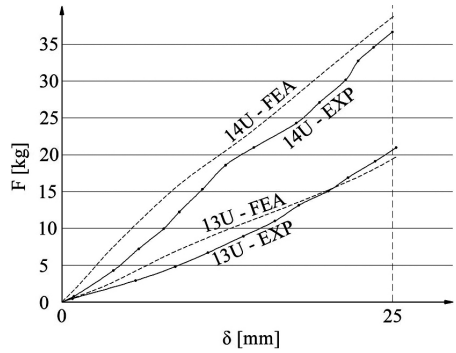

Fig. 6. Load-displacement relationship for specimens 13U and 14U

The comparison of the numerical results analyzed individually for each model, as in Figures 5 and 6, or collectively in Tables 4 and 5, confirms the initial conclusion from the experimental tests that the 2+0 fastener arrangement results in higher values of the stiffness C_D. In the experimental tests, the values obtained were 1.67 to 2.93 times higher for gravity loading and 1.37 to 2.21 times higher for uplift loading. In the case of the values obtained from the numerical simulations, this ratio was more than 2.0 in any case.

Table 4. Numerical results for gravity loading

Test specimen	F **[N]**	K **[N/mm]**	K_A **[N/mm]**	$C_{D,\mathrm{FEA}}$ **[Nm/m]**	**Ratio**	$C_{D,\mathrm{FEA}}/C_{D,\mathrm{EXP}}$
(1)	**(2)**	**(3)**	**(4)**	**(5)**	**(6)**	**(7)**
1G	165.1	8.26	9.16	366	2.73	1.11
2G	417.1	20.85	24.99	1000		1.04
3G	133.3	6.67	7.21	288	2.55	0.81
4G	323.3	16.17	18.41	737		1.12
5G	116.7	4.67	5.84	365	2.53	1.08
6G	259.6	10.38	14.78	924		1.48
7G	100.3	4.01	4.80	300	2.24	0.89
8G	207.8	8.31	10.76	673		1.19
9G	255.8	12.79	15.09	604	2.55	0.87
10G	589.3	29.46	38.46	1538		1.28
11G	209.6	10.48	11.89	476	2.49	0.98
12G	484.6	24.23	29.65	1186		1.49
13G	170.4	6.82	9.64	602	2.20	0.95
14G	329.6	13.18	21.18	1324		1.17
15G	152.4	6.10	8.14	509	2.08	0.80
16G	289.2	11.57	16.94	1059		0.85
17G	181.5	9.07	10.16	407	2.59	1.02
18G	435.9	21.79	26.31	1052		1.24
19G	144.4	7.22	7.86	314	2.49	0.94
20G	341.3	17.07	19.57	783		1.27
21G	125.5	5.02	6.39	399	2.37	1.23
22G	264.3	10.57	15.11	944		1.23
23G	108.8	4.35	5.29	331	2.07	1.17
24G	211.2	8.45	10.97	686		1.14
					Average:	**1.10**
					COV:	**0.17**

A slightly larger dispersion of C_D values in the case of experimental tests may result from the difficulty in placing the fastener exactly in the middle of the width of the purlin flange, because at the time of joining, the purlin flange is hidden under the trapezoidal sheet.

Table 5. Numerical results for uplift loading

Test specimen	F [N]	K [N/mm]	K_A [N/mm]	$C_{D,\mathrm{FEA}}$ [Nm/m]	**Ratio**	$C_{D,\mathrm{EXP}}/C_{D,\mathrm{FEA}}$
(1)	**(2)**	**(3)**	**(4)**	**(5)**	**(6)**	**(7)**
1U	171.0	8.55	9.21	368	2.65	0.86
2U	430.1	21.50	24.43	977		1.12
3U	136.7	6.84	7.24	290	2.48	0.73
4U	327.5	16.38	17.99	719		0.87
5U	122.5	4.90	5.80	363	2.50	0.84
6U	277.4	11.10	14.50	906		1.01
7U	104.0	4.16	4.78	299	2.26	0.71
8U	220.9	8.84	10.83	677		0.76
9U	274.1	13.70	15.47	619	2.58	0.92
10U	652.9	32.64	39.89	1596		1.40
11U	221.4	11.07	12.17	487	2.47	0.96
12U	517.3	25.86	30.12	1205		1.21
13U	190.4	7.62	10.04	628	2.22	0.92
14U	378.6	15.14	22.29	1393		1.08
15U	164.2	6.57	8.26	517	2.12	0.73
16U	320.3	12.81	17.49	1093		1.12
17U	190.2	9.51	10.32	413	2.58	0.76
18U	464.1	23.20	26.61	1064		1.13
19U	154.8	7.74	8.26	330	2.38	0.77
20U	354.6	17.73	19.62	785		0.92
21U	132.9	5.31	6.38	399	2.39	0.77
22U	288.7	11.55	15.25	953		0.97
23U	113.0	4.52	5.26	329	2.12	0.75
24U	226.5	9.06	11.15	697		0.72
					Average:	**0.92**
					COV:	**0.20**

After performing all the tests, the distance of the fastener location from the center line was additionally measured. Although the test set-up was prepared in laboratory conditions, these imperfections were even up to 3.5 mm. It should be noted that in numerical models such an imperfection will not occur, which is why the spread of C_D values is smaller.

6. Comparison with the eurocode 3-1-3 formula

As the values of stiffness C_D obtained from numerical simulations confirm the validity of the results obtained in the experimental tests, they can be compared with the C_D values calculated on the basis of the Eurocode 3-1-3 provisions. As mentioned earlier in Section 2, in a limited number of cases, the stiffness C_D can be calculated from two formulae recommended by Eurocode 3-1-3 [1]: a simple one ($130p$) and a complex one developed by Lindner [11] and later modified by Vrany [13]. The experimental C_D values are compared with those determined on the basis of the Eurocode formula in Tables 6 and 7 for gravity loading and in Tables 8 and 9 for uplift loading.

Table 6. Results based on Eurocode 3-1-3 for 1+1 fastener arrangement and gravity loading

Test specimen	$C_{D,\mathrm{EC3}}$ **[Nm/m]**	$C_{D,\mathrm{EC3}}/C_{D,\mathrm{EXP}}$	$C_{D,130p}$ **[Nm/m]**	$C_{D,130p}/C_{D,\mathrm{EXP}}$	$C_{D,\mathrm{EC3,new}}$ **[Nm/m]**	$C_{D,\mathrm{EC3,new}}/C_{D,\mathrm{EXP}}$
(1)	**(2)**	**(3)**	**(4)**	**(5)**	**(6)**	**(7)**
1G	473	1.44	489	1.49	381	1.16
3G	368	1.04	489	1.38	297	0.84
5G	473	1.40	489	1.44	381	1.13
7G	368	1.09	489	1.44	297	0.88
9G	783	1.13	489	0.70	632	0.91
11G	610	1.25	489	1.00	492	1.01
13G	783	1.24	489	0.77	632	1.00
15G	610	0.96	489	0.77	492	0.77
17G	547	1.37	492	1.23	441	1.10
19G	426	1.27	492	1.46	343	1.02
21G	547	1.68	492	1.51	441	1.36
23G	426	1.51	492	1.75	343	1.22
	Average:	**1.28**		**1.25**		**1.03**
	COV:	**0.16**		**0.27**		**0.16**

It is clear that the current restrictions on the applicability of the formula in Section 10.1.5.2 of Eurocode 3-1-3 [1] made it possible to determine the stiffness value C_D only for gravity loading with the 1+1 fastener arrangement. In the other cases, i.e. with the uplift or gravity loading, but with two fasteners in every second trough, no values of the coefficient C_{100} are given. In such cases, the value of C_D cannot be determined or the simple $130p$ formula must be used.

Thus, in Tables 6 to 9, in column 2, the values of stiffness C_D determined according to the Eurocode 3-1-3 formula in Section 10.1.5.2 are presented, omitting the fact that the diameter of the fasteners used in the test was 5 mm, and not 6.3 mm as required. However,

Table 7. Results based on Eurocode 3-1-3 for 2+0 fastener arrangement and gravity loading

Test specimen	$C_{D,\mathrm{EC3}}$ [Nm/m]	$C_{D,\mathrm{EC3}}/C_{D,\mathrm{EXP}}$	$C_{D,130p}$ [Nm/m]	$C_{D,130p}/C_{D,\mathrm{EXP}}$	$C_{D,\mathrm{EC3,new}}$ [Nm/m]	$C_{D,\mathrm{EC3,new}}/C_{D,\mathrm{EXP}}$
(1)	**(2)**	**(3)**	**(4)**	**(5)**	**(6)**	**(7)**
2G	–	–	489	0.51	732	0.76
4G	–	–	489	0.74	570	0.87
6G	–	–	489	0.78	732	1.17
8G	–	–	489	0.87	570	1.01
10G	–	–	489	0.41	1213	1.01
12G	–	–	489	0.61	944	1.19
14G	–	–	489	0.43	1213	1.07
16G	–	–	489	0.39	944	0.76
18G	–	–	492	0.58	847	1.00
20G	–	–	492	0.80	659	1.07
22G	–	–	492	0.64	847	1.10
24G	–	–	492	0.82	659	1.10
	Average:	**–**		**0.63**		**1.01**
	COV:	**–**		**0.26**		**0.14**

Table 8. Results based on Eurocode 3-1-3 for 1+1 fastener arrangement and uplift loading

Test specimen	$C_{D,\mathrm{EC3}}$ [Nm/m]	$C_{D,\mathrm{EC3}}/C_{D,\mathrm{EXP}}$	$C_{D,130p}$ [Nm/m]	$C_{D,130p}/C_{D,\mathrm{EXP}}$	$C_{D,\mathrm{EC3,new}}$ [Nm/m]	$C_{D,\mathrm{EC3,new}}/C_{D,\mathrm{EXP}}$
(1)	**(2)**	**(3)**	**(4)**	**(5)**	**(6)**	**(7)**
1U	–	–	489	1.14	458	1.07
3U	–	–	489	1.23	356	0.89
5U	–	–	489	1.13	458	1.06
7U	–	–	489	1.16	356	0.85
9U	–	–	489	0.73	758	1.13
11U	–	–	489	0.96	590	1.16
13U	–	–	489	0.72	758	1.12
15U	–	–	489	0.69	590	0.83
17U	–	–	492	0.91	529	0.98
19U	–	–	492	1.14	412	0.96
21U	–	–	492	0.96	529	1.03
23U	–	–	492	1.12	412	0.94
	Average:	**–**		**0.99**		**1.00**
	COV:	**–**		**0.19**		**0.11**

Table 9. Results based on Eurocode 3-1-3 for 2+0 fastener arrangement and uplift loading

Test specimen	$C_{D,EC3}$ [Nm/m]	$C_{D,EC3}/C_{D,EXP}$	$C_{D,130p}$ [Nm/m]	$C_{D,130p}/C_{D,EXP}$	$C_{D,EC3,new}$ [Nm/m]	$C_{D,EC3,new}/C_{D,EXP}$
(1)	**(2)**	**(3)**	**(4)**	**(5)**	**(6)**	**(7)**
2U	–	–	489	0.56	870	0.99
4U	–	–	489	0.59	677	0.82
6U	–	–	489	0.54	870	0.97
8U	–	–	489	0.55	677	0.76
10U	–	–	489	0.43	1440	1.26
12U	–	–	489	0.49	1121	1.13
14U	–	–	489	0.38	1440	1.12
16U	–	–	489	0.50	1121	1.15
18U	–	–	492	0.52	1005	1.07
20U	–	–	492	0.58	783	0.92
22U	–	–	492	0.50	1005	1.02
24U	–	–	492	0.51	783	0.81
	Average:	**–**		**0.51**		**1.00**
	COV:	**–**		**0.11**		**0.15**

in [15] it was already proved that the value of the diameter of the sheet-to-purlin fastener does not significantly affect the final value of the stiffness C_D, so this limitation was considered irrelevant. In those design cases where the stiffness C_D could be determined, the ratio of the values obtained using the Eurocode to the experimental values ranged from 0.96 to 1.68 with the average value being 1.28 (see column 3 in Table 6). Thus, in most cases, the current guidelines overestimated the value of C_D or could not be used to determine its value according to that part of Eurocode 3-1-3.

In order to reconfirm what was already stated in [14], i.e. that values of stiffness C_D obtained from the $130p$ formula are far from stiffness values obtained in real tests, they were also listed in column (4). Their average ratio to the experimental values varies from case to case between 0.51 and 1.25. The use of this formula in engineering practice is simple, but it gives a very inaccurate estimation of the stiffness C_D and may lead to calculating an incorrect buckling resistance of cold-formed Z-purlins restrained by trapezoidal sheeting.

Finally, column (6) contains values of stiffness C_D calculated according to the Eurocode 3-1-3 provisions. In all cases, where it was not possible to determine the value of stiffness C_D due to the lack of the value of coefficient C_{100} in [1] the following values were proposed:

– C_{100} = 4800 Nm/m – for the 2+0 fastener arrangement under gravity loading (Table 7),
– C_{100} = 3000 Nm/m – for the 1+1 fastener arrangement under uplift loading (Table 8),
– C_{100} = 5700 Nm/m – for the 2+0 fastener arrangement under uplift loading (Table 9).

For gravity loading and the 1+1 fastener arrangement (Table 6), a new modified value of C_{100} = 2500 Nm/m was proposed instead of the value given in [1] equal 3100 Nm/m.

In all these cases, the average ratio of the estimated stiffness values $C_{D,EC3,new}$ (taking into account the new value of the rotational coefficient C_{100}) to the values from the experimental tests $C_{D,EXP}$ was equal or close to 1.0.

7. Buckling resistance of the z-purlin

When comparing the results of the experimental tests for two different arrangements of fasteners (1+1 and 2+0), significant differences in the obtained C_D values can be observed. It is possible to obtain more than twice higher rotational restraint of a cold-formed Z-purlin given by trapezoidal sheeting with the use of the same number of fasteners in connection but in a different arrangement. However, in engineering practice, the most important thing is how it affects the buckling resistance of cold-formed Z-purlins restrained by trapezoidal sheeting.

Using the procedure according to Eurocode 3-1-3, the ultimate limit load $q_{Ed,\max}$ for a continuous purlin of 6.0 m span with no or one intermediate anti-sag bar was calculated satisfying the inequality defined by Eq. (7.1).

$$\frac{1}{\chi_{LT}}\left(\frac{M_{y,Ed}}{W_{\text{eff},y}}+\frac{N_{Ed}}{A_{\text{eff}}}\right)+\frac{M_{fz,Ed}}{W_{fz}}\leq\frac{f_y}{\gamma_{M1}} \tag{7.1}$$

where: A_{eff} – the effective area of the cross-section for only uniform compression, $W_{\text{eff},y}$ – the effective section modulus of the section for bending about the $y-y$ axis only, W_{fz} – the gross elastic section modulus of the free flange plus the contributing part of the web for bending about the $z-z$ axis.

The calculations were carried out only for purlins Z250x68x2.0 and trapezoidal sheeting T40 × 0.7 (specimens 13G, 14G, 13U and 14U from Table 1). The values of the rotational stiffness C_D from the experimental tests obtained for the 1+1 and 2+0 fastener arrangements were used. While verifying the ultimate limit state, in each case, the compression normal force of N_{Ed} = 10 kN was assumed. The maximum value of the ultimate limit load $q_{ult.Ed}$ was calculated for the yield stress equal to f_y = 320 MPa, which was determined in a static tensile test of steel. The results are presented in Fig. 7. In both figures, the higher values of the ultimate limit load refer to the case where there is an intermediate anti-sag bracing, while the lower values are obtained in the absence of such a bracing.

It can be stated that for the analyzed cross-sections of purlins and sheeting, changing the fasteners arrangement from 1+1 to 2+0 causes an increase of 12.6% in the buckling resistance of a continuous purlin without intermediate anti-sag bars. For purlins with an intermediate bracing, differences in the ultimate limit load $q_{Ed,\max}$ are not so significant (1.6%), despite large differences in the C_D values. At the same time, it can be seen that the use of the $130p$ formula to estimate the value of C_D results in an underestimation of the purlin's buckling resistance (in the analyzed cases, up to 6.3% for gravity loading and 7.3% for uplift loading).

It should be clearly explained that the increase in the buckling resistance presented above was obtained for specific cross-sections of the trapezoidal sheet and the Z-profile and for a continuous purlin with a span of 6 m. For other profile geometries or other static schemes of the purlin, other values of the differences may occur and each case should be considered individually.

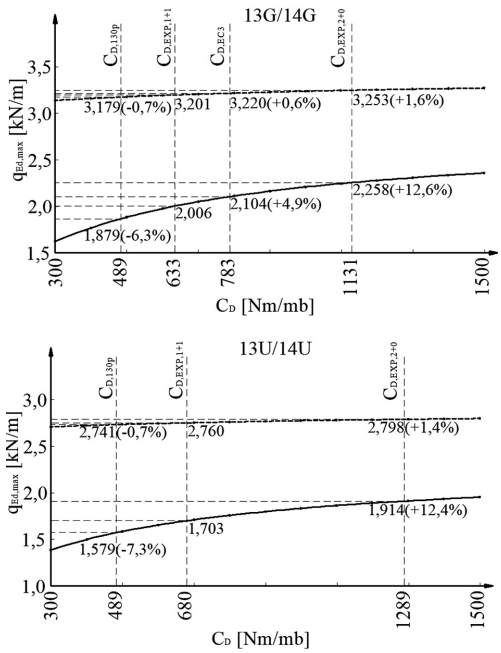

Fig. 7. Relationship between the ultimate limit load $q_{Ed,\max}$ and the stiffness C_D

8. Conclusions

Based on the research, it can be concluded that the use of the same number of fasteners between the trapezoidal sheeting and the Z-purlin, but in the 2+0 arrangement instead of the traditional 1+1 arrangement, increases the values of the rotational stiffness C_D. When using second-generation trapezoidal sheeting with stiffening ribs in the middle of the trough width, it is justified to use two purlin-to-sheeting fasteners in every second trough near the webs. Such an arrangement of fasteners in experimental tests gave 1.63 to 2.93 times higher values of the rotational stiffness C_D under gravity loading (Table 2) and 1.37 to 2.21 times higher values under uplift loading (Table 3).

It was also shown that an increase in the stiffness value C_D has a positive effect on the final buckling resistance of cold-formed Z-purlins restrained by trapezoidal sheeting. This beneficial effect will depend to a large extent on the static scheme of the purlin itself; however, in the case of the analyzed continuous purlin with a span of 6.0 m without intermediate anti-sag bracings, an increase in the ultimate limit load was up to 12.6% (Fig. 7).

After analyzing the results obtained from the experimental tests, the new values of the rotational coefficient C_{100} for cases not covered by Eurocode 3-1-3 were presented (the 1+1 fastener arrangement with the uplift loading and the 2+0 fastener arrangement with both loading cases). In addition, a modification of this coefficient for the 1+1 fastener arrangement under gravity loading was proposed.

References

[1] EN 1993-1-3 Eurocode 3 – Design of steel structures. Part 1–3: General rules – Supplementary rules for cold-formed members and sheeting. European Committee for Standardization, 2006.

[2] B. W. Schafer and T. Pekoz, "Computational modeling of cold-formed steel: characterizing geometric imperfections and residual stresses", *Journal of Constructional Steel Research*, vol. 47, no. 3, pp. 193–210, 1998, doi: 10.1016/S0143-974X(98)00007-8.

[3] G. J. Hancock, "Design for distortional buckling of flexural members", *Thin-Walled Structures*, vol. 27, no. 1, pp. 3–12, 1997, doi: 10.1016/0263-8231(96)00020-1.

[4] J. P. Papangelis, G. J. Hancock, and N. S. Trahair, "Computer design of cold-formed C- and Z-section purlins", *Journal of Constructional Steel Research*, vol. 46, no. 1–3, pp. 169–171, 1998, doi: 10.1016/s0143-974x(98)00085-6.

[5] J. Bródka, M. Broniewicz, and M. Giżejowski, *Kształtowniki gięte: poradnik projektanta*. Arkady, 2006.

[6] ENV 1993-1-3 Eurocode 3 – Design of steel structures. Part 1–3: General rules – Supplementary rules for cold-formed members and sheeting. European Committee for Standardization, 1996.

[7] J. Lindner and T. Gregull, "Torsional restraint coefficients of profiled sheeting", in *Proc. Of International Association for Bridge and Structural Engineering, Colloquium Stockholm.* Zürich, Switzerland, 1986, pp. 161–168.

[8] J. Lindner, "Stabilisierung von Trägern durch Trapezbleche", *Stahlbau,* vol. 56, no. 1, pp. 9–15, 1987.

[9] J. Lindner and T. Gregull, "Drehbettungswerte für Dachdeckungen mit untergelegter Wärmedämmung", *Stahlbau,* vol. 58, no. 6, pp. 173–179, 1989.

[10] J. Lindner and F. Groeschel, "Drehbettungswerte für die Profilblechbefestigung mit Setzbolzen bei unterschiedlich grossen Auflasten", *Stahlbau,* vol. 65, no. 6, pp. 218–224, 1996.

[11] J. Lindner, "Restraint of beams by trapezoidally sheeting using different types of connection", in *Stability and Ductility of Steel Structures*, T. Usami and Y. Itoh, Eds. Elsevier, 1998, pp. 27–36, doi: 10.1016/B978-008043320-2/50004-6.

[12] T. Vrany, "Rotační podepření tenkostěnné ocelové vaznice krytinou", Ph.D. Dissertation, Czech Technical University of Prague, Praha, 2002.

[13] T. Vrany, "Effect of loading on the rotational restraint of cold-formed purlins", *Thin-Walled Structures,* vol. 44, no. 12, pp. 1287–1292, 2006, doi: 10.1016/j.tws.2007.01.004.

[14] M. Gajdzicki and J. Goczek, "Numerical Determination of Rotational Restraint of Cold-formed Z-purlin According to EC3", *International Journal of Steel Structures,* vol. 15, no. 3, pp. 633–645, 2015, doi: 10.1007/s13296-015-9010-x.

[15] M. Gajdzicki and J. Goczek, "Influence of Sheet-to-purlin Fastener Properties on the Rotational Restraint of Cold-formed Z-purlins", *International Journal of Steel Structures,* vol. 17, no. 2, pp. 711–721, 2017, doi: 10.1007/s13296-017-6025-5.

[16] F. Wang, H. Zhang, J. Yang, L. Bai, and C. Ren, "Numerical studies of the rotational stiffness of purlin–sheeting system", *International Journal of Steel Structures,* vol. 18, no. 3, pp. 719–733, 2018, doi: 10.1007/s13296-018-0048-4.

[17] Y. Zhang, J. Xue, X. Song, and Q. Zhang, "Numerical Parametric Analysis of the Ultimate Loading-Capacity of Channel Purlins with Screw-Fastened Sheeting", *International Journal of Steel Structures,* vol. 18, pp. 1801–1817, 2018, doi: 10.1007/s13296-018-0080-4.

[18] M. Gajdzicki, "Sheet-to-purlin fasteners arrangement and the value of rotational restraint of cold-formed Z-purlins", *Journal of Constructional Steel Research,* vol. 151, pp. 185–193, 2018, doi: 10.1016/j.jcsr.2018.09.028.

[19] I. Balazs, J. Melcher, and A. Belica, "Experimental investigation of torsional restraint provided to thin walled purlins by sandwich panels under uplift load", *Procedia Engineering,* vol. 161, pp. 818–824, 2016, doi: 10.1016/j.proeng.2016.08.718.

[20] K. Ciesielczyk and R. Studziński, "Experimental and numerical investigation of stabilization of thin-walled Z-beams by sandwich panels", *Journal of Constructional Steel Research,* vol. 133, pp. 77–83, 2017, doi: 10.1016/j.jcsr.2017.02.016.

[21] H. Yang and F. Bai, "Buckling behavior of cold-formed C/Z-section purlins incorporating the effects of diaphragm and the screw location", *Advances in Structural Engineering,* vol. 23, no. 6, pp. 1114–1128, 2020, doi: 10.1177/1369433219888739.

[22] C. Zhao, J. Yang, F. Wang, et al., "Rotational stiffness of cold-formed steel roof purlin–sheeting connections", *Engineering Structures*, vol. 59, pp. 284–297, 2014, doi: 10.1016/j.engstruct.2013.10.024.

[23] Z. Nagy, B. Bács, A. Kelemen, A. Sánduly, Ö. Nagy, and B. Lőrincz, "Rafter-purlin connection stiffness impact on the stress skin effect of corrugated sheet claddings", *Thin-Walled Structures*, vol. 185, 2023, doi: 10.1016/j.tws.2023.110615.

[24] C. Ren, X. Zhao, and Y. Chen, "Buckling behavior of partially restrained cold-formed steel zed purlins subjected to transverse distributed uplift loading", *Engineering Structures*, vol. 114, pp. 14–24, 2016, doi: 10.1016/j.engstruct.2016.01.048.

[25] K. Reszut, I. Szewczak, P. Różyło, and M. Guminiak, "Impact of numerical modelling of kinematic and static boundary conditions on stability of cold-formed sigma beam", *Archives of Civil Engineering*, vol. 69, no. 2, pp. 311–323, 2023, doi: 10.24425/ace.2023.145269.

Sztywność obrotowa podparcia sprężystego płatwi typu z połączonej z poszyciem z blachy trapezowej z usztywnieniem pośrednim

Słowa kluczowe: płatew profilowana na zimno, łącznik płatew-poszycie, sztywność obrotowa, stężanie przeciwskrętne

Streszczenie:

Obudowa z blach trapezowych mocowanych bezpośrednio do płatwi z kształtownika typu Z profilowanych na zimno jest powszechnie stosowana w systemach dachowych hal magazynowych. Rozwój technologii profilowania blach stalowych spowodował wprowadzenie blach trapezowych o coraz bardziej skomplikowanych przekrojach, w których występują liczne podłużne usztywnienia pośrednie (profile drugiej generacji). Jednakże za tym rozwojem nie podążają przepisy normowe zawarte w Eurokodzie 3-1-3, zgodnie z którymi należy określić wartość sztywności obrotowej podparcia sprężystego płatwi C_D. W przepisach tych nie tylko brakuje wytycznych dla blach trapezowych drugiej generacji, ale są one również bardzo ograniczone w przypadku blach bez dodatkowych usztywnień (blachy pierwszej generacji). Niestety prowadzi to do sytuacji, w których projektanci konstrukcji stalowych zmuszeni są ignorować ograniczenia opisanych w nich zasad, nie mając pewności, czy obliczona wartość nośności wyboczeniowej pasa swobodnego płatwi jest prawidłowa.Zgodnie z tymi zapisami sztywność C_D można również wyznaczyć z bardzo prostego wzoru (130p), w którym wartość sztywności zależy tylko od parametru p, czyli liczby łączników blacha-płatew na metr długości płatwi. Ze względu na swoją prostotę wzór ten jest częściej stosowany w praktyce inżynierskiej, jednak daje wyniki zawsze po stronie niebezpiecznej (zawyżającej nośność płatwi), co pokazano we wcześniejszych badaniach przeprowadzonych przez Autora i dlatego należy go usunąć z Eurokodu 3-1-3. We wcześniejszych badaniach również zostało wykazane, że zastosowanie dwóch łączników blacha-płatew w co drugiej fałdzie blachy trapezowej skutkuje większymi wartościami sztywności obrotowej C_D. Jednakże w badaniach tych wykorzystano wyłącznie blachy trapezowe pierwszej generacji, w których nie zastosowano podłużnych usztywnień pośrednich. W opisanych w niniejszej pracy badaniach eksperymentalnych zastosowano blachę trapezową drugiej generacji z żebrami usztywniającymi na środnikach i w dolinie fałdy. W Eurokodzie 3-1-3 płatew w miejscu połączenia z blachą trapezową można uznać za stężoną w płaszczyźnie poszycia, jeśli jest mocowana za pomocą wkrętów samogwintujących w każdej lub w co drugiej fałdzie blachy. W drugim przypadku blacha zapewnia pięciokrotnie mniejszą sztywność na ścinanie (0,2S). W przypadku blach

trapezowych drugiej generacji, gdzie w środku fałdy znajduje się wewnętrzne usztywnienie podłużne, konieczne jest przesunięcie łącznika w jedną lub drugą stronę. Dlatego też w niniejszej pracy zdecydowano się przeanalizować różnice w wartościach sztywności obrotowej C_D płatwi typu Z, gdy po jednym łączniku znajduje się w każdej fałdzie obok usztywnienia pośredniego (układ 1+1) lub dwa łączniki w co drugiej fałdzie, ale przesunięte do środników blachy trapezowej (układ 2+0). W tym celu przygotowano 48 próbek badawczych, różniących się przekrojem kształtownika profilowanego na zimno, geometrią blachy trapezowej oraz kierunkiem obciążenia. W badaniach eksperymentalnych zastosowano łączniki o średnicy 5,0 mm i podkładki uszczelniające o średnicy 14 mm. Łączniki umieszczono w odległości 10 mm od podłużnego usztywnienia pośredniego doliny blachy w układzie 1+1 i 10 mm od środników blachy trapezowej w układzie 2+0. Wyniki badań eksperymentalnych zestawiono w Tablicach 2 i 3, a następnie zweryfikowano je przy użyciu symulacji numerycznych w programie Abaqus, wykorzystując do tego zaawansowane modele MES opracowane wcześniej przez Autora. Porównanie wyników numerycznych zestawionych zbiorczo w Tabelach 4 i 5, potwierdza wstępny wniosek z badań eksperymentalnych, że zastosowanie dwóch łączników w pobliżu środników blachy trapezowej, ale w co drugiej fałdzie, powoduje zwiększenie wartości sztywności C_D. W badaniach eksperymentalnych uzyskane wartości były od 1,67 do 2,93 razy wyższe dla obciążeń grawitacyjnych i od 1,37 do 2,21 razy wyższe dla obciążeń odrywających. W przypadku wartości uzyskanych z symulacji numerycznych współczynnik ten w każdym przypadku był większy od 2,0. Nieco większy rozrzut wartości C_D w przypadku badań doświadczalnych może wynikać z trudności w umieszczeniu łącznika dokładnie w środku szerokości pasa górnego płatwi, gdyż w momencie wykonywania połączenia pas płatwi jest ukryty pod blachą trapezową. Po wykonaniu wszystkich badań doświadczalnych, zmierzono odległość położenia łącznika od linii środkowej i mimo, że stanowiska badawcze były przygotowane w warunkach laboratoryjnych, odchyłka ta dochodziła nawet do 3,5 mm. W modelach numerycznych taka niedoskonałość nie wystąpi, dlatego rozrzut wartości C_D jest mniejszy.Następnie wartości doświadczalne sztywności C_D porównano z wartościami wyznaczonymi na podstawie dwóch wzorów zalecanych przez Eurokod 3-1-3: prostego (130p) i złożonego opracowanego przez Lindnera, a później zmodyfikowanego przez Vrany'ego. Obecne ograniczenia stosowania wzoru z punktu 10.1.5.2 Eurokodu 3-1-3 umożliwiły wyznaczenie wartości sztywności C_D tylko dla obciążeń grawitacyjnych z układem łączników 1+1 (w każdej fałdzie). W pozostałych przypadkach, tj. przy obciążeniu unoszącym lub grawitacyjnym, ale przy dwóch łącznikach, w co drugiej fałdzie, nie ma określonych wartości współczynnika C_{100}, koniecznych do wyznaczenia całkowitej wartości sztywności C_D. W takich przypadkach projektant nie jest w stanie określić poprawnej wartości sztywności obrotowej koniecznej do wyznaczenia nośności wyboczeniowej płatwi lub musi zastosować prosty wzór 130p, który prowadzi do zawyżonych wartości nośności płatwi. Zestawione wyniki w Rozdziale 6 pozwoliły na zaproponowanie nowych wartości współczynnika $C_{100,}$ dzięki którym zapisy normy 3-1-3 mogą być stosowane w zdecydowanie większej liczbie sytuacji projektowych. Na koniec przedstawiono wyniki analizy wpływu wartości sztywności C_D na nośność wyboczeniową pasa swobodnego płatwi, dla wybranych rozpiętości płatwi. W skrajnym przypadku dla płatwi bez stężeń pośrednich pasa swobodnego w przęśle, różnice w warunku nośności wzrastały o 12,6% przy zastosowaniu układu łączników 2+0, w porównaniu do standardowego układu 1+1.

Received: 2023-10-03, Revised: 2023-11-21